Excited atomic energy levels in protactinium by resonance ionization spectroscopy

Pascal Naubereit,* Tina Gottwald, Dominik Studer, and Klaus Wendt
Institute of Physics, University of Mainz, 55128 Mainz, Germany

(Received 18 May 2018; published 10 August 2018)

We present high-resolution data of the single-excitation spectrum of protactinium, reaching slightly beyond the first-ionization threshold. Within this work, more than 1500 energy levels are recorded in different excitation energy ranges below 50 000 cm^{-1}. Our experimental results show that the tabulated data in the literature severely underestimate the density of states particularly regarding the highly excited spectral range.

DOI: 10.1103/PhysRevA.98.022505

I. INTRODUCTION

Laser resonance ionization spectroscopy is an utterly versatile technique for investigations on the atomic shell [1] as well as for gaining knowledge of the characteristics of the nuclear structure and properties of rare species [2,3]. It has been used throughout the Periodic Table of elements for high-precision studies up to fermium; therefore, it is denotable that protactinium ($Z = 91$) is the only actinide below element number 100, the actinide element fermium, for which no spectroscopic measurements were performed until today [4]. To be more precise, it is, besides a few chalcogenic, halogenic, and refractory elements, which are known to be rather difficult to investigate with laser spectroscopic methods, the only element at all [4]. The only ever laser-ionized protactinium beam, without advanced spectroscopy, was demonstrated in [5]. In order to prepare comprehensive studies on the atomic system as well as for nuclear structure research via resonance ionization spectroscopy it is necessary to identify and investigate efficient optical excitation schemes to provide highly resolved spectra.

Here we present high-resolution spectroscopic data of the excitation spectrum of protactinium. Protactinium is also one of the very few remaining elements in the Periodic Table for which the fundamental atomic quantity of the first-ionization potential has not yet been precisely measured [6]; a value of $E_{IP} = 49\,000(110)$ cm^{-1} [6.075(14) eV] has been inferred from systematic comparison to the other actinides and isoelectronic lanthanides [5]. This shortcoming is not only due to the unpleasant radiological and chemical properties of protactinium, which make sample preparation and the production of a stable atomic beam, as required in such experiments, very complicated. Also the complexity of its atomic spectrum has so far prevented a conclusive analysis towards a determination of the ionization potential via Rydberg convergences: Rydberg series could not be identified due to the exceptionally high level density of other excited states below the ionization potential. The level density in the protactinium spectrum even exceeds that of most other actinide and the isoelectronic lanthanide elements. Both groups exhibit several open shells and numerous "active" electrons. The electronic structure of Pa with an even-parity ground-state configuration $7s^2 5f^2 6d$ involves in relativistic notation $7s_{1/2}$, $5f_{5/2,7/2}$, $6d_{3/2,5/2}$, and additionally $7p_{1/2,3/2}$ orbitals. These $N = 32$ possible single-electron states for each individual of the $n = 5$ active valence electrons in Pa lead to $\sim(N)^n/n! \approx 2.8 \times 10^5$ possible electron configurations [7,8]. Given this rough estimate, we note that the 156 even and 494 odd energy levels available in the literature [9] are by far not complete but strongly suggest unobserved levels particularly situated at increasing excitation energies. Furthermore, no level at all has been tabulated so far for excitation energies above 34 500 cm^{-1} (38 500 cm^{-1}) for even (odd) parity [9].

In the measurements presented here, we studied far more than 2000 resonances in the bound spectrum of the Pa atom, covering selected energy ranges and states of different total angular momentum and parity. Making use of multistep laser resonance ionization spectroscopy [10,11] with wide-range tunable Ti:sapphire lasers, extensive scans on resonances and level positions in different energy ranges of the spectrum were recorded.

II. EXPERIMENTAL SETUP

For a fully resonant two-step (three-step) excitation, two (three) lasers of the Mainz titanium:sapphire laser system, involving second-harmonic generation (SHG) and third-harmonic generation (THG), were used. The standard Z-shaped cavity lasers according to [12] have a typical linewidth of 4(1) GHz (fundamental) to 6(1) GHz (SHG) and 7(2) GHz (THG), respectively, and provide an average output power of tunable laser light between 2 and 4 W. The power output for frequency-doubled and -tripled lasers is somewhat lower, depending on wavelength and adjustment, lying somewhat below 500 mW. A Ti:sapphire laser with a grating-assisted resonator served as the scanning laser for spectroscopy. This laser type, a modified development of [13], allows continuous scanning without mode-hop covering almost the complete Ti:sapphire gain range from 650 to 1000 nm. Due to wavelength selection via a refraction grating, a linewidth below 2(1) GHz, with a slightly reduced output power of approximately 2 W, can be achieved. All lasers have a typical pulse length between 30 and 90 ns. A commercially available frequency-doubled diode-pumped solid-state Nd:YAG laser (Photonics Industries

*naubereit@uni-mainz.de

 ©2018 American Physical Society

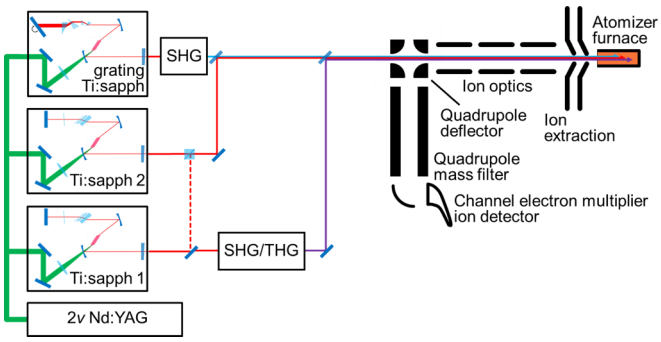

FIG. 1. Sketch of the experimental setup including the Ti:sapphire laser system on the left-hand side and the mass spectrometer system on the right-hand side. For details, see the text.

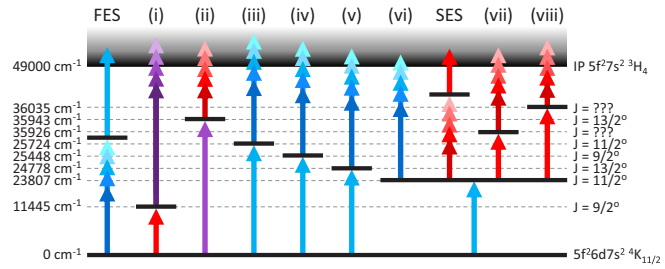

FIG. 2. Compilation of excitation schemes for resonance ionization spectroscopy used for protactinium within this work. For further details see the text.

DM 100-532) at 10-kHz repetition rate delivers the necessary pump power of 10–15 W for each Ti:sapphire laser. For more detailed information on the laser system used, see, for example, [14] and references therein.

Figure 1 gives an overview of the apparatus; the laser system is depicted schematically on the left-hand side. The right-hand side shows a sketch of the low-energy mass spectrometer system, the Mainz Atomic Beam Unit. The lasers are guided inside, anticollinearly overlapped to the atomic beam into the atomizer furnace. Samples of typically 10^{14} atoms of ^{231}Pa dissolved in nitric acid are crystallized on a zirconium foil acting as reduction agent, which is afterward placed in the atomizer furnace. The resistively heated graphite furnace with an inner diameter of 2.2 mm and a length of 50 mm is internally fully lined by tantalum to prevent formation of PaC on the walls [15]. After vaporization at temperatures above the melting point of protactinium at 1568 °C and reduction of PaO, PaO_2, and especially the high-stable Pa_2O_5 molecules, the Pa atoms are ionized via stepwise excitation by the laser radiation, drift towards the exit hole of the furnace, and are extracted and accelerated with low electric fields on the order of 10 V/mm. After passing ion optics for beam shaping, the ions are separated from evaporated neutral species by bending the ion beam in a 90° electrostatic quadrupole deflector. Subsequent mass separation with a radio-frequency quadrupole mass filter separates the ^{231}Pa ions from other ionic species before the ions are detected by a channel electron multiplier in single-ion counting mode.

Several effects, e.g., Doppler broadening and broadening due to the laser linewidth, increase the width of measured resonances compared to their natural linewidth, but an achieved resolution in the range below 20 GHz (FWHM) for most transitions is still well suited for resolving individual states with high precision. However, we have to mention that some transitions into autoionizing resonances may exceed this value by far.

III. WIDE-RANGE HIGH-RESOLUTION LASER RESONANCE IONIZATION SPECTROSCOPY

The overall scanning range of the Ti:sapphire laser system is spanning only 1500 cm^{-1}. Thus, we have probed the spectrum of Pa I in several ranges, from 23 600 cm^{-1} up to the first-ionization potential and slightly above. We used several excitation schemes in order to investigate different total angular momenta of both parities. Figure 2 gives an overview on all investigated excitation schemes. Herein, the arrows in out-fading colors depict the scanned step and the color itself gives a hint to the laser wavelength range in each step. Levels where the configuration or a J value is indicated can also be found in the literature [9]. All schemes where the ionization step was scanned are labeled in roman numerals, while FES (SES) describes the search for a first (second) excitation step using a nonresonant ionization step. All schemes start from the even-parity atomic ground-state configuration $7s^25f^26d\ ^4K_{11/2}$ located at zero energy (0 cm^{-1}). To ensure that the excitation does not start from a thermally populated fine-structure component slightly above the lowest ground state, found at 825.42, 1618.3, or 1978.2 cm^{-1} (odd parity), we choose transitions into energy levels, listed in the literature with an unambiguously assigned value for the total angular momentum [9]. Based on the selection rule $\Delta J = \pm 1, 0$, fulfilled for every optically allowed dipole transition, and the known J value of the initial state, a range of just three [five for the three-step schemes (vii) and (viii)] neighboring J values can be inferred for our measured resonances. Beyond that, some total angular momenta of resonances could be assigned by comparing several scans of excitation schemes with different J values (see the Supplemental Material [16]).

The uncertainties of all energy levels measured in this work are calculated in a similar way. The statistical error accounts for fitting errors in the first place. A smaller contribution is ascribed to the data acquisition, which slightly shifts the spectra depending on scan direction and speed. The latter can be easily corrected, but result in a small contribution to the overall statistical uncertainty. The systematic uncertainty is produced by the wavelength measurement using a High Finesse WS6-600 wavelength meter. Fast statistical scattering is averaged out due to a rather low scanning speed and the fitting procedure. Long-term drifts and absolute measurement uncertainties are covered within the specified 1σ absolute accuracy. Thus it must be applied for every measured wavelength contributing to the total excitation energy of each level.

In the following sections level energies are compared to the levels available in the literature [9]. According to [17–19], i.e., the primary resources of [9], the resonance energies might be slightly shifted due to variations in excitation probability of the underlying hyperfine-structure components. As a consequence, we added half of the hyperfine-structure width given in [9] as additional uncertainty of the literature values for

TABLE I. Compilation of energy ranges, parity, total angular momenta, and number of atomic transitions in protactinium as identified in the different excitation schemes: FES, SES, and (i)–(viii). Energy levels available in literature [9] are given for comparison.

Scheme	Energy range (cm^{-1})	Parity	Range of J	Transitions
FES	23600, . . . , 26000	odd	$\frac{9}{2}, \ldots, \frac{13}{2}$	88
SES	35800, . . . , 36400	even	$\frac{9}{2}, \ldots, \frac{13}{2}$	32
(i)	48600, . . . , 49100	even	$\frac{7}{2}, \ldots, \frac{11}{2}$	215
(ii)	48900, . . . , 49500	even	$\frac{11}{2}, \ldots, \frac{15}{2}$	67
(iii)	48100, . . . , 49500	even	$\frac{9}{2}, \ldots, \frac{13}{2}$	424
(iv)	49200, . . . , 50000	even	$\frac{7}{2}, \ldots, \frac{11}{2}$	159
(v)	48600, . . . , 49500	even	$\frac{11}{2}, \ldots, \frac{15}{2}$	119
(vi)	48100, . . . , 49400	even	$\frac{9}{2}, \ldots, \frac{13}{2}$	432
(vii)	47900, . . . , 49100	odd	$\frac{7}{2}, \ldots, \frac{15}{2}$	472
(viii)	48500, . . . , 49700	odd	$\frac{7}{2}, \ldots, \frac{15}{2}$	316
[9]	0, . . . , 34500	even	$\frac{3}{2}, \ldots, \frac{17}{2}$	156
[9]	2000, . . . , 38500	odd	$\frac{3}{2}, \ldots, \frac{17}{2}$	494

comparison. In cases where no width was indicated, we took the half mean of all given widths as the uncertainty.

Table I gives a compilation of the number of individual resonances which were determined in the ten different two- and three-step excitation schemes given in Fig. 2. We have to mention that in this compilation several schemes contain a number of identical energy levels. For a complete list of levels observed in this work we refer to the Supplemental Material [16]. For comparison, the numbers of hitherto tabulated levels in the literature [9] are included in Table I, covering a range about half of the excitation energies up to the first-ionization potential. For most of these levels, parity and total angular momentum have been assigned.

A. Search for first and second excitation steps

There is no simple procedure to experimentally distinguish between excitations starting from the ground state or, alternatively, from a thermally populated state located slightly above. Already at a moderate atomizer furnace temperature of 1500 °C, the state at 825.42 cm^{-1} has a population ratio of 20%. Another problem appears since for the two-step schemes (i)–(vi) the radiation of the first and the scanning laser could swap regarding the consecutive steps of the ladder of excitation. Correspondingly, the scanning laser might excite the atoms into a first excited state and the actual first-step laser serves for nonresonant ionization. The following procedure is used to circumvent these difficulties during data analysis: At first, for every detected resonance, two energies are calculated, one expecting the transition to start from the ground state and the other expecting the transition to start from the thermally populated state at 825.42 cm^{-1}. To the energies obtained (note that every transition is now doubly existent), a set of five rules is applied.

(a) The available literature data found in [9] are correct. That means matching energies in any scan for either value, starting from the ground state or from the thermally excited state, are considered as first excited states, as long as the total angular momentum is suitable.

(b) All transitions that appear in more than one scan are considered as leading into a first excited state; again this is valid for both excitations considered as starting from the ground state or from the thermally populated state.

(c) If for one resonance neither the transition starting from the ground state nor from the thermally populated state fulfills rule (a) or (b), this resonance line is considered as leading into a second excited state. In contrast, the remaining transitions in the FES scheme are considered to lead into first excited states.

(d) For any transition matching one of the rules above, the corresponding "other" transition, i.e., starting either from the ground state or from the thermally populated state, is discarded. This ensures that for each resonance in a spectrum only one energy level remains in the end.

(e) The few remaining resonances that fulfill more than one of the rules above and resonances where transitions starting both from the ground state and from the thermally populated state match a rule are treated as special cases, which are analyzed separately.

After this separation procedure the total excitation energy for every transition was calculated. In total 239 first excited states were found and are displayed in Table III in the Supplemental Material [16]. Obeying rule (a), 72 of them can directly be found in [9] and thus a total angular momentum can be assigned. For two of them, numbers 145 and 159 in Table III in the Supplemental Material [16], the range of possible total angular momenta given in [9] could be limited to the value $\frac{11}{2}$. Rule (b) can be applied to 167 levels, while for 67 of them the energies appear only in scans starting from the ground state *or* from the thermally populated state. These 67 level energies are somewhat unreliable as we cannot state explicitly from which state the excitation starts; they are thus labeled with a question mark in the Supplemental Material [16]. For these presently detected energy levels, there is a chance between 47% (at 1500 °C) and 35% (at 2000 °C) for excitation from the ground state, depending on the temperature in the source region, and between about 20% (at 1500 °C) and 18% (at 2000 °C) from the state at 825.42 cm^{-1}. For the other 100 levels it was possible to restrict the range for the total angular momentum. One transition with an energy of $27\,812.68(19)_{stat}(1)_{sys}$ cm^{-1} is supposed to start from the thermally populated odd state at 1978.22 cm^{-1} leading to an even-parity level, while all other transitions lead to odd-parity levels. Level number 119 in the table for odd levels (Table III of the Supplemental Material [16]), would match a level at $25\,891.71(1)_{stat}(1)_{sys}$ cm^{-1} from [9] if we consider an excitation from the state at 825.42 cm^{-1}, but should not be accessible due to the assigned total angular momentum of $\frac{15}{2}$ [9]. Despite our confidence in the correctness of the energy level assignments, there is still a non-negligible possibility that a second-step transition coincidentally matches the energy of a first excited state.

Figure 3 shows the scan of the search for a first excitation step in the lower trace. The poor statistics especially at lower excitation energies in this scan are caused by low laser powers and an almost depleted sample.

In a further step of the excitation scheme development we scanned with an infrared laser to reach an energy range around 36 000 cm^{-1} by a two-step excitation. Therefore, we

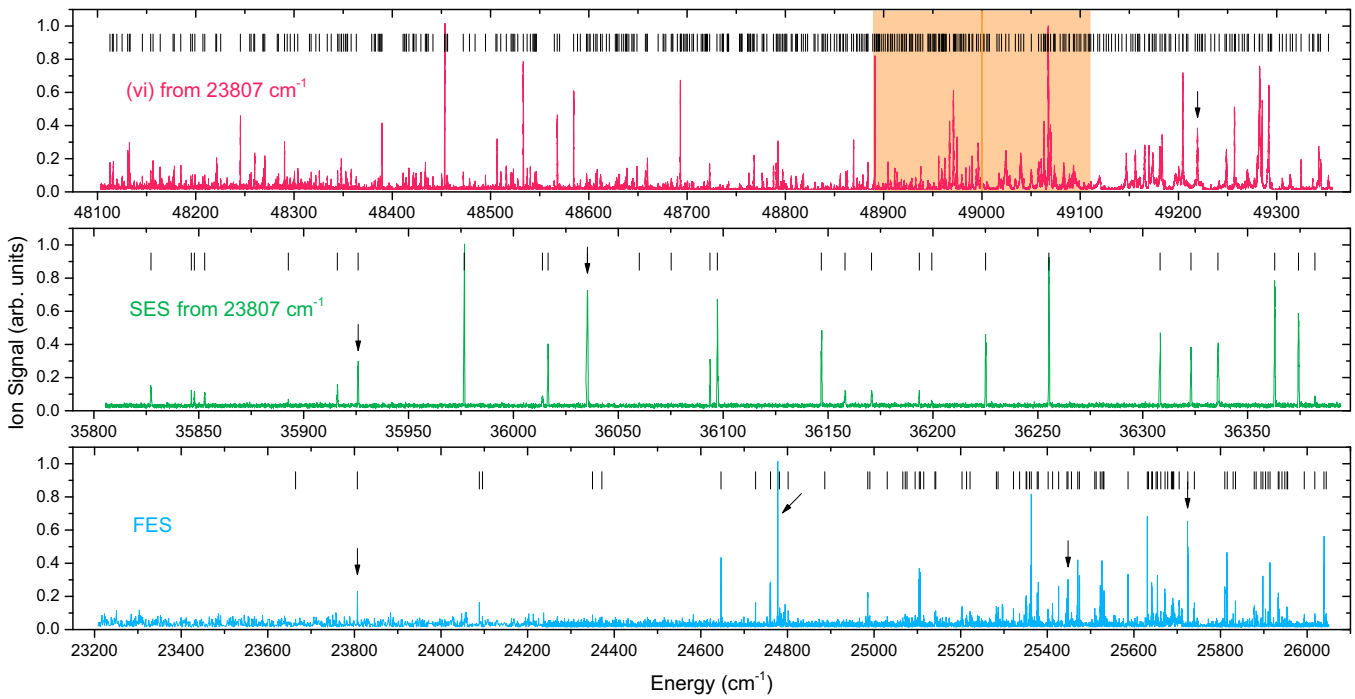

FIG. 3. Different wide-range scans with normalized count rates. The energy scale shows the calculated total excitation energy. Every resonance is indicated by a black bar above the spectra, while arrows indicate resonances used in the various excitation schemes of Fig. 2 or for the frequency scans of Fig. 4. The bottom graph shows the search for a first excitation step, the middle the search for a second excitation step, and the top the scan of scheme (vi). In this scan, the orange line represents the value for the expected ionization potential of $E_{\mathrm{IP}} = 49\,000(110)\ \mathrm{cm}^{-1}$ with its uncertainty range visualized as the light orange area.

used the odd-parity energy level at 23 807 cm^{-1} with a total angular momentum of $J = \frac{11}{2}$ as the first excited state. Of all the levels with sufficient excitation probability and assigned J value detected in the FES scheme, this state has one of the lowest energies [9]. A nonresonant one-color two-photon ionization above an estimated ionization potential of $E_{\mathrm{IP}} = 49\,000(110)\ \mathrm{cm}^{-1}$ is not possible. A range of $J = \frac{9}{2}, \ldots, \frac{13}{2}$ for the second excited states is accessible. Additional to the laser for excitation into the first excited state and the scanning laser, a third laser, also operating in the infrared range, was utilized to ionize from the second excited states nonresonantly. To ensure that the measured resonances represent second excited states, and do not accidentally coincide with alternative first excited states, the scan was repeated with three different nonresonant ionization steps. Consequently, only levels appearing in at least two scans were accepted as second excited states. Those 28, out of 32 in total, energy levels are listed in the compilation for even-parity energy levels in Table I of the Supplemental Material [16]. The middle trace of Fig. 3 shows a typical scan of the SES scheme.

B. Two-step excitation schemes

In addition to the previously described schemes, we investigated highly excited energy levels of protactinium via the six different two-step excitation schemes (i)–(vi) in energy ranges around 49 000 cm^{-1} situated below to slightly beyond the expectation for the first-ionization potential. The first excited states for schemes (i) and (ii) are taken from the literature [9], while for the others a state found via the FES scheme was used. All of the first excited states can additionally be found in [9] and have a clearly assigned value for the total angular momentum, which once again results in a range of three consecutive J values for the measured resonances within the second step. The upper trace of Fig. 3 shows the very dense scan of scheme (vi) as an example for the highly excited spectra.

Schemes (i) and (ii) use laser light in the ultraviolet range for either the scanning or the first-step excitation, respectively. In both cases the sum frequency generation technique was applied [20]. For the scanning uv laser two individual lasers are needed. One intracavity frequency-doubled laser [21] at a fixed wavelength is sum frequency mixed with the scanning laser running in fundamental wavelength operation. The uv laser with fixed wavelength, as needed for scheme (ii), is a frequency-tripled laser, where only one laser is frequency doubled and then again mixed with its own fundamental wavelength output. Unfortunately, for scheme (i) we cannot check if the resonances found are first-step transitions, because we did not perform first-step searches in that energy range due to the experimental challenge for the further excitation steps nor did the literature cover this energy range. In addition, the number of detected energy levels is very low compared to other schemes of the same parity and energy range, as depicted in Table I. Due to this fact, a presumably low transition strength for the first excitation step may cause many resonances of scheme (ii) to remain undetected. Nevertheless, none of the detected transitions of scheme (ii) seems to belong to first excited states comparing the fundamental energies of the scanning laser to the literature data [9].

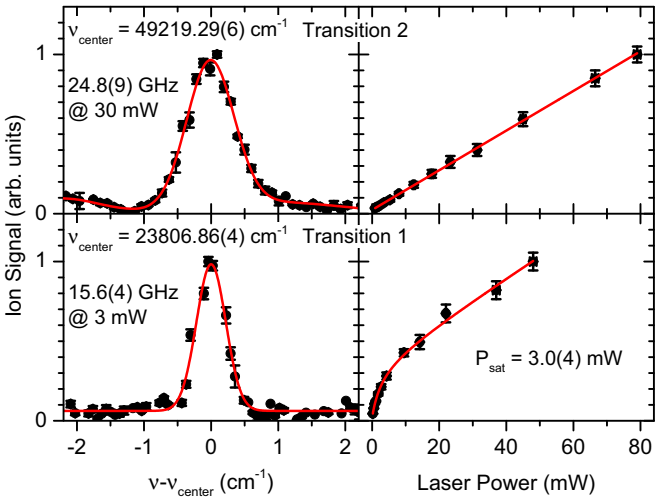

FIG. 4. Frequency scans and saturation curves for the two-step excitation scheme (vi). Here the second transition yields for an autoionizing state at 49 219 cm^{-1}, hence the saturation shows linear behavior. Both linewidths and the saturation power of the first transition are noted in the graph. See the text for further details.

Applying the rules described in Sec. III A, the entirety of second excited even-parity energy levels with their own range of J values found via the two-step schemes (i)–(vi) was finally compared after calculating their total excitation energy. They are given in Table II in the Supplemental Material [16] for even-parity energy levels. For levels matching each other within their uncertainties, the weighted averages are given as the final level energy. Wherever possible, the values of the total angular momenta were limited due to a procedure of exclusion.

Figure 4 shows frequency scans and saturation curves of one exemplary pair of transitions measured along scheme (vi), where the second step populates an autoionizing state at an excitation energy of 49 219 cm^{-1}. On the left-hand side of this resonance, the tailing from a neighboring resonance is visible. In order to optimize the ionization efficiency, the saturation behavior was investigated for every transition [14]. The resulting saturation curve of the first transition shows a clear saturation behavior followed by a somewhat unexpected linear slope. Due to the high level density in protactinium, a second-step transition might lead nearly resonantly to an energy level located around $2 \times 23\,807$ cm^{-1} followed by nonresonant ionization. The second transition exhibits a linearly increasing count rate with laser power due to a nonsaturated autoionizing resonance. The resonance scans on the left show nonsaturated peak shapes, namely, a Gaussian profile for transition 1 and a rather symmetric Fano profile for transition 2, respectively. Note that the linewidth for the first transition with a width of 15.6 GHz is much broader than most of the other transitions measured below the expected first-ionization potential. This fact is ascribed to the relatively broad hyperfine structure involved: A width of 11.5 GHz is given in [9].

C. Three-step excitation schemes

Schemes (vii) and (viii) are three-step excitation schemes, where the transition from the ground state into the $J = \frac{11}{2}$ state at 23 807 cm^{-1} was used as the first excitation step. The second excited state for both schemes was initially detected via scans using the SES scheme, as shown in the center trace of Fig. 3. For these states with energies of 35 926 and 36 035 cm^{-1}, respectively, a range for the total angular momentum of $J = \frac{9}{2}, \ldots, \frac{13}{2}$ is suitable. Consequently, this results in a range of $J = \frac{7}{2}, \ldots, \frac{15}{2}$, which is permitted for energy levels detected by the scanned third excitation step. Note that the third excited states may also lead into one of three consecutive J values. Since we do not know the J value of the intermediate second excited state, the range of these three values is comprised within the interval of five consecutive J values given. First and second excited states are chosen in such a way that direct nonresonant ionization from the first excited state with photons of the third laser is very unlikely to occur without a necessary intermediate resonant laser step. Nonetheless, other combinations could be possible, but are not expected to be strong. To verify this statement, we performed an exclusion scan, where the intermediate second-step laser was blocked. The remaining resonances in this scan were compared with schemes (vii) and (viii), here with a 3σ systematic uncertainty, and matching levels were directly sorted out from the scans for schemes (vii) and (viii). Similar to the two-step scans, also a comparison of possible transitions from the ground state with the literature levels [9] was performed during which further matching transitions were again sorted out. After these procedures, we are confident that the energies of the levels given for schemes (vii) and (viii) in the table for odd-parity energy levels in the Supplemental Material [16] are correct. The odd-parity levels in this list were also compared with their total energy and if two levels matching each other within their uncertainties were found, the weighted averages were calculated.

IV. CONCLUSION AND OUTLOOK

An extensive search for resonance ionization schemes was performed in protactinium. We identified far more than 2000 resonances and found about 1500 so far undocumented energy levels. Most of these levels are located around the expected value for the first-ionization potential at 49 000(110) cm^{-1} and cover both parities and several different total angular momenta. The achieved resolution is limited by the experimental linewidth of typically below 20 GHz for levels below the first-ionization potential with significantly broader autoionizing resonances above. Some of the detected levels indicate signs of broad hyperfine splittings which need to be investigated more thoroughly. In this work every resolved peak was fitted separately, because it was not possible to define whether it is an individual level or a hyperfine component. Since we have not found clear Rydberg series in any of the spectra, we have investigated the level structure more deeply in order to nevertheless extract a reasonably precise value for the first-ionization potential applying different analytical approaches. In parallel, we evaluated this extraordinary complex atomic structure concerning indications of intrinsic quantum chaos through analyzing the measures of spectral fluctuations (cf. [22,23]) and compared our findings to recently published simulated data [24] and theoretical predictions as given by the random matrix theory.

ACKNOWLEDGMENTS

The authors want to thank N. Trautmann and P. Thörle-Pospiech from the Mainz Institute of Nuclear Chemistry for preparation of the protactinium samples. P.N. gratefully acknowledges the Carl-Zeiss-Stiftung and D.S. the EU through ENSAR2 RESIST (Grant No. 654002) for financial support.

[1] M. Laatiaoui *et al.*, Nature (London) **538**, 495 (2016).
[2] K. M. Lynch *et al.*, Phys. Rev. C **97**, 024309 (2018).
[3] C. Granados *et al.*, Phys. Rev. C **96**, 054331 (2017).
[4] P. Campbell, I. D. Moore, and M. R. Pearson, Prog. Part. Nucl. Phys. **86**, 127 (2016).
[5] K. Wendt, T. Gottwald, C. Mattolat, and S. Raeder, Hyperfine Interact. **227**, 55 (2014).
[6] A. Kramida, Y. Ralchenko, J. Reader, and NIST ASD Team (2015), NIST Atomic Spectra Database, version 5.3, available at http://physics.nist.gov/asd (accessed 29 September 2016) (National Institute of Standards and Technology, Gaithersburg, 2015).
[7] V. V. Flambaum, A. A. Gribakina, G. F. Gribakin, and M. G. Kozlov, Phys. Rev. A **50**, 267 (1994).
[8] V. A. Dzuba and V. V. Flambaum, Phys. Rev. Lett. **104**, 213002 (2010).
[9] J. Blaise and J.-F. Wyart, Energy Levels and Atomic Spectra of Actinides, available at http://web2.lac.u-psud.fr/lac/Database/Contents.html (accessed 29 September 2016) (TIC, Paris, 1992).
[10] R. V. Ambartzumian and V. S. Letokhov, Appl. Opt. **11**, 354 (1972).
[11] V. S. Letokhov and V. I. Mishin, Opt. Commun. **29**, 168 (1979).
[12] S. Rothe, B. A. Marsh, C. Mattolat, V. N. Fedosseev, and K. Wendt, J. Phys.: Conf. Ser. **312**, 052020 (2011).
[13] A. Teigelhöfer, P. Bricault, O. Chachkova, M. Gillner, J. Lassen, J. P. Lavoie, R. Li, J. Meißner, W. Neu, and K. D. A. Wendt, Hyperfine Interact. **196**, 161 (2010).
[14] P. Naubereit, J. Marín-Sáez, F. Schneider, A. Hakimi, M. Franzmann, T. Kron, S. Richter, and K. Wendt, Phys. Rev. A **93**, 052518 (2016).
[15] C. Keller, Angew. Chem. Int. Edit. **5**, 23 (1966).
[16] See Supplemental Material at http://link.aps.org/supplemental/10.1103/PhysRevA.98.022505 for all energy levels found within this work. The Resonances detected via the various excitation schemes have been compared in order to extract the positions of the energy levels. They are grouped in four tables for even and odd as well as low and high energy. Where possible, J-values or ranges of J-values have been deduced. Levels with an uncertain energy position are marked with "?". For more information on the determination of energy positions, see full text of the article.
[17] A. Giacchetti, J. Opt. Soc. Am. **56**, 653 (1966).
[18] E. W. T. Richards, I. Stephen, and H. S. Wise, Spectrochim. Acta B **23**, 635 (1968).
[19] J. Blaise, A. Ginibre, and J. F. Wyart, Z. Phys. A **321**, 61 (1985).
[20] Y. B. Band, C. Radzewicz, and J. S. Krasinski, Phys. Rev. A **49**, 517 (1994).
[21] V. Sonnenschein, I. D. Moore, I. Pohjalainen, M. Reponen, S. Rothe, and K. Wendt, JPS Conf. Proc. **6**, 030126 (2015).
[22] F. Haake, *Quantum Signatures of Chaos*, Springer Series in Synergetics Vol. 54 (Springer, Berlin, 2013).
[23] T. Guhr, A. Müller-Groeling, and H. A. Weidenmüller, Phys. Rep. **299**, 189 (1998).
[24] A. V. Viatkina, M. G. Kozlov, and V. V. Flambaum, Phys. Rev. A **95**, 022503 (2017).